Suplemento de la Revista Mexicana de Física **4** 021128 (2023) 1–5

An electron-muon collider: what can be probed with it?

A. O. Bouzas and F. Larios

Departamento de Física Aplicada, CINVESTAV-Mérida,
Apartado Postal 73, 97310 Mérida, Yucatán, México.

Received 15 May 2023; accepted 13 September 2023

Collisions of electrons against muons provide a very clean environment for many beyond SM signals. We consider the case of two-to-two flavor changing processes that are absent in the SM. The sensitivity of the $e\mu$ collider to the four-fermion dimension six operators is about the same order of magnitude as the one based on low energy measurements.

Keywords: Electron-muon; two-to-two process.

DOI: https://doi.org/10.31349/SuplRevMexFis.4.021128

1. Introduction

The collision of muons vs. electrons to search for physics beyond the Standard Model has been considered for some time. For example, Lepton Flavor Violation (LFV) at very low energy collisions of a few GeV (Center of Mass energy) was presented in Ref. [1] back in 1997, and even up to present times there is significant interest in new physics effects of the muon lepton that can be probed at the low energy MUonE machine [2]. Nevertheless, high energy collisions of order 1 or more TeV have also been considered of interest back in the same year 1997 [3]. On the other hand, studies that were not based on LFV were presented in Refs. [4–7]. Recently, as the prospect of a muon collider has become more compelling due to the very high energies that could be achieved [8], the interest on high energy $e\mu$ collisions has been brought up again by [9] in 2020 and by [10] in 2021. Clearly, observation of LFV processes is a topic of prime interest: in Ref. [9] a heavy Z' with generic couplings to leptons was considered and it is found that the $e^-\mu^+ \to e^+\mu^-$ process that violates flavor number by two units would give better constraints on the $Z'\mu e$ coupling than the low energy rare muon decays. Similarly, in Ref. [10] the authors propose the construction of a high energy $e\mu$ collider that could be a better probe of, not only a flavor changing coupling like $H\mu e$, but even of the SM Hbb vertex as compared to the LHC.

In this talk, we refer to a study on two-to-two processes at a μ^+e^- collider for center-of-mass (CM) energies of order a few TeV [11]. In Ref. [11] we consider four-fermion $\mu e f\bar{f}$ effective interactions and obtain limits from a non-observation of $f\bar{f}$ final states in two-to-two interactions. In addition, we consider the dimension 6 flavor changing magnetic dipole $e\mu\gamma$ coupling as well as the dimension 8 contact term $e\mu\gamma\gamma$ for the $e^-\mu^+ \to \gamma\gamma$ annihilation process. In this case we have done a signal vs background analysis at detector level to further validate our prediction on the sensitivity.

2. Two-to-two processes

At tree level, the SM predicts only two kinds of these production processes: elastic $e^-\mu^+ \to e^-\mu+$ and $e^-\mu^+$ annihilation into two neutrinos; as shown in Fig. 1. Emission of an additional photon is the only possibility for two-to-three processes and the $e^-\mu^+$ collider thus provides such a clean environment that in Ref. [10] it is shown that even a process that does not involve flavor violation like Higgs production and decay to $b\bar{b}$ can be a competitive probe of the Hbb coupling.

With the idea of taking advantage of the (almost) absence of SM backgrounds for two-to-two processes we turn our attention to four-fermion couplings that involve the $e\mu$ pair and two other leptons or quarks [11]. These couplings can be probed with low energy measurements like $\mu \to e\gamma$, $\mu^- \to e^-e^+e^-$ and $\mu A \to eA$ conversion reactions in nuclei [12].

The framework that we use is the SM effective Lagrangian with dimension six operators that is known as the *Warsaw* basis [13]. There are 13 four-fermion operators that involve the $e\mu$ pair:

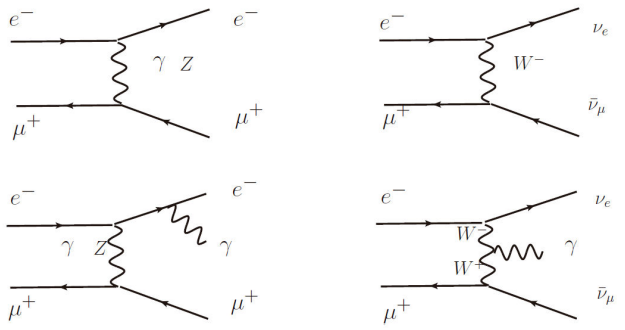

FIGURE 1. The tree level SM processes in $e^-\mu^+$ collisions with 2 or 3 final state particles.

$$
\begin{aligned}
Q_{lq}^{(1)} &= \bar{l}_p\gamma_\mu l_r\bar{q}_s\gamma^\mu q_t, \qquad Q_{lq}^{(3)} = \bar{l}_p\gamma_\mu\tau^k l_r\bar{q}_s\gamma^\mu\tau^k q_t,\\
Q_{ll} &= \bar{l}_p\gamma_\mu l_r\bar{l}_s\gamma^\mu l_t, \qquad Q_{ee} = \bar{e}_p\gamma_\mu e_r\bar{e}_s\gamma^\mu e_t,\\
Q_{eu} &= \bar{e}_p\gamma_\mu e_r\bar{u}_s\gamma^\mu u_t, \qquad Q_{ed} = \bar{e}_p\gamma_\mu e_r\bar{d}_s\gamma^\mu d_t,\\
Q_{le} &= \bar{l}_p\gamma_\mu l_r\bar{e}_s\gamma^\mu e_t, \qquad Q_{lu} = \bar{l}_p\gamma_\mu l_r\bar{u}_s\gamma^\mu u_t,\\
Q_{ld} &= \bar{l}_p\gamma_\mu l_r\bar{d}_s\gamma^\mu d_t, \qquad Q_{qe} = \bar{q}_p\gamma_\mu q_r\bar{e}_s\gamma^\mu e_t,\\
Q_{ledq} &= \bar{l}_p e_r\bar{d}_s q_t, \qquad Q_{lequ}^{(1)} = \bar{l}_p^j e_r\epsilon_{jk}\bar{q}_s^k u_t,\\
Q_{lequ}^{(3)} &= \bar{l}_p^j\sigma^{\mu\nu}e_r, \epsilon_{jk}\bar{q}_s^k\sigma_{\mu\nu}u_t\ .
\end{aligned}
\tag{1}
$$

The $prst$ are fermion family indices that we have set as $21jj$ for $j = 1, 2, 3$ that is all the charged leptons ($e\mu\tau$), the down quarks (dsb) and the up quarks (uc). (Top quark production belongs to the case of two-to-four processes.) For left helicity massless fermions we have l and q doublets, whereas right helicity fermions are denoted as e, u and d [13]. We then show four types of cross sections depending on the helicities of the colliding e^- and μ^+.

A general expression of the cross section for colliding beams with some degree of polarization is written as:

$$
\begin{aligned}
\sigma_{Pe^-P\mu^+} = &\frac{1+\mathcal{P}_{e^-}}{2}\frac{1+\mathcal{P}_{\mu^+}}{2}\,\sigma_{++}\\
&+\frac{1-\mathcal{P}_{e^-}}{2}\frac{1-\mathcal{P}_{\mu^+}}{2}\,\sigma_{--}\\
&+\frac{1+\mathcal{P}_{e^-}}{2}\frac{1-\mathcal{P}_{\mu^+}}{2}\,\sigma_{+-}\\
&+\frac{1-\mathcal{P}_{e^-}}{2}\frac{1+\mathcal{P}_{\mu^+}}{2}\,\sigma_{-+}\ .
\end{aligned}
\tag{2}
$$

The dimension 6 operators of Eq. (1) yield the following cross sections:

$$
\begin{aligned}
\frac{\sigma_{++}}{\sigma_{1234}} &= 4|C_{le}|^2 + N_c|C_{ledq}|^2\\
&\quad + N_c|C_{lequ}^{(1)}|^2 + \frac{16}{3}N_c|C_{lequ}^{(3)}|^2,\\
\frac{\sigma_{+-}}{\sigma_{1234}} &= \frac{4}{3}|C_{ee}|^2 + \frac{4}{3}N_c|C_{eu}|^2\\
&\quad + \frac{4}{3}N_c|C_{ed}|^2 + \frac{4}{3}N_c|C_{qe}|^2,\\
\frac{\sigma_{-+}}{\sigma_{1234}} &= \frac{4}{3}|C_{ll}|^2 + \frac{4}{3}|C_{le}|^2 + \frac{4}{3}N_c|C_{lq}^{(1)}|^2\\
&\quad + \frac{4}{3}N_c|C_{lq}^{(3)}|^2 + \frac{4}{3}N_c|C_{lu}|^2 + \frac{4}{3}N_c|C_{ld}|^2\ .
\end{aligned}
\tag{3}
$$

Where the σ_{--} term does not appear for the flavor index assignment 2111, but the operators that generate σ_{++} would also generate σ_{--} with the assignment 1211.

By requiring that the value of a C_Q coefficient be enough to yield the minimum 0.04fb of production cross section, we obtain the following lower limits for $E_e = 100$, $E_\mu = 3000$ GeV:

TABLE I. The ratio of limits based on low energy observables and limits from the $e\mu$ collider.

C_Q	C^{Low}/C^{Coll}	C^{Low}/C^{Coll}
	$e^-\mu^+ \to \mu^-\mu^+$	$e^-\mu^+ \to \tau^-\tau^+$
C_{ll}	0.34	0.69
C_{ee}	0.34	0.69
C_{le}	1.20	1.19
	$e^-\mu^+ \to s\bar{s}$	$e^-\mu^+ \to b\bar{b}$
$C_{lq}^{(1)}$	0.96	1.50
$C_{lq}^{(3)}$	0.37	1.50
C_{ld}	1.19	1.50
C_{qe}	1.19	1.50
C_{ed}	0.95	1.51
C_{ledq}	5.8×10^{-3}	0.19
	$e^-\mu^+ \to c\bar{c}$	$---$
C_{lu}	0.53	
C_{eu}	0.54	
$C_{lequ}^{(1)}$	0.05	
$C_{lequ}^{(3)}$	6.4×10^{-4}	

$$
\begin{aligned}
C_{ll}\ ,\ C_{ee} &\ \geq\ 2.88\times10^{-2},\\
C_{ledq}\ , C_{lequ}^{(1)} &\ \geq\ 1.92\times10^{-2},\\
C_{le}\ ,\ C_{lu}\ , C_{ld}\ ,\ C_{qe} &\ \geq\ 1.66\times10^{-2},\\
C_{eu}\ ,\ C_{ed}\ , C_{lq}^{(1)}\ ,\ C_{lq}^{(3)} &\ \geq\ 1.66\times10^{-2},\\
C_{lequ}^{(3)} &\ \geq\ 0.83\times10^{-2}.
\end{aligned}
\tag{4}
$$

In Table I, we show the comparison between these limits and those based on low energy measurements. It should be noted that for the latter, the $\mu A \to eA$ conversion in nuclei is the most sensitive probe [12]. Without this $\mu A \to eA$ input the limits in Ref. [12] would be much weaker and the relative sensitivity shown in Table I would favor the potential of the $e\mu$ collider. The limits for the first family fermions are not shown in Table I but can be seen in Ref. [11]. They turn out to be two or three orders of magnitude weaker than those reported in Ref. [12].

In addition to the dimension six operators, we have also included some of the four-fermion dimension eight operators that were also addressed in Ref. [14]:

$$
\begin{aligned}
Q_{le}^{(8)} &= \bar{l}_p H e_r\bar{l}_s H e_t, \qquad Q_{Tle}^{(8)} = \bar{l}_p H\sigma^{\mu\nu}e_r\bar{l}_s H\sigma_{\mu\nu}e_t,\\
Q_{leqd1}^{(8)} &= \bar{l}_p H e_r\bar{q}_s H d_t, \qquad Q_{leuq}^{(8)} = \bar{l}_p H e_r\bar{u}_s\tilde{H}^\dagger q_t,\\
Q_{leqd3}^{(8)} &= \bar{l}_p H\sigma^{\mu\nu}e_r\bar{q}_s H\sigma_{\mu\nu}d_t,
\end{aligned}
\tag{5}
$$

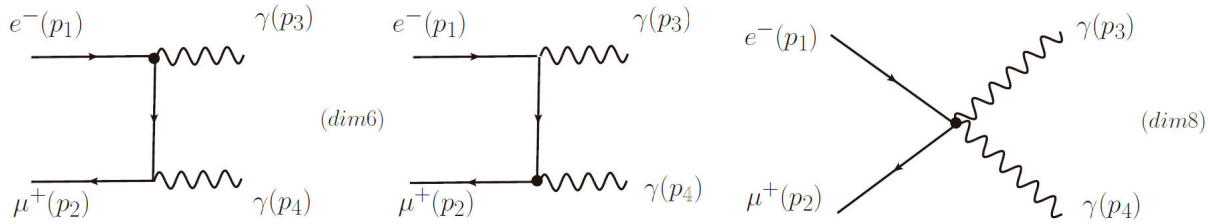

FIGURE 2. Diagrams for the signal process $e^-\mu^+ \to \gamma\gamma$.

where H is the Higgs doublet [14]. The dimension 8 operators of Eq. (5) yield the following cross sections:

$$\frac{\sigma_{++}}{\sigma_{1234}}(e_R^- e_L^+) = \frac{v^4}{4\Lambda^4}\left(|C_{le}^{(8)}|^2 + N_c|C_{leqd1}^{(8)}|^2 + N_c|C_{leuq}^{(8)}|^2 + \frac{16}{3}N_c|C_{leqd3}^{(8)}|^2 + \frac{16}{3}|C_{Tle}^{(8)}|^2\right)$$

$$\frac{\sigma_{++}}{\sigma_{1234}}(e_L^- e_R^+) = \frac{v^4}{4\Lambda^4}\left(\frac{1}{3}|C_{le}^{(8)}|^2 + \frac{112}{3}N_c|C_{Tle}^{(8)}|^2\right). \quad (6)$$

The scale Λ was chosen to be 4 TeV in Ref. [11][i]. In this case the relative sensitivity is much lower for the $e\mu$ collider, see Table 4 in Ref. [11]. In the following section, we consider the other case of two-to-two processes where the final state is a pair of photons.

3. The process $e^-\mu^+ \to \gamma\gamma$

We now consider the magnetic dipole operators Q_{uB} and Q_{uW} of the *Warsaw* basis. We are only interested in the effective couplings that involve the photon, so let us focus on the FCNC magnetic dipole operator that arises from a combination of Q_{uB} and Q_{uW}:

$$Q_{eA} = \bar{l}_\mu \sigma^{\mu\nu} e_e H F_{\mu\nu} \ , \quad (7)$$

where l_μ is the left-handed doublet with the muon and e_e the right-handed singlet of the electron. In Fig. 2 we show the corresponding Feynman diagrams. Another contribution comes from the dimension 8 operator[ii]

$$Q_{eAA} = \bar{l}_\mu e_e H F^{\mu\nu} F_{\mu\nu} \ . \quad (8)$$

This operator generates an effective $e\mu\gamma\gamma$ coupling as shown in Fig. 2. We have two chiral versions for each operator: (Q_{eAL},Q_{eAR}) and (Q_{eAAL}, Q_{eAAR}) referring to left-handed and right-handed electron, respectively [11].

Both operators give rise to amplitudes that do not depend on angles:

$$\sum|\mathcal{M}|^2 = \left(|C_{eAL}|^2 + |C_{eAR}|^2\right) e^2 \frac{v^2}{\Lambda^4} 48s + \left(|C_{eAAL}|^2 + |C_{eAAR}|^2\right) \frac{v^2}{\Lambda^8} 4s^3. \quad (9)$$

They yield the total cross sections:

$$\begin{aligned}\sigma_{--} + \sigma_{++} &= \left(|C_{eAL}|^2 + |C_{eAR}|^2\right) \frac{3e^2v^2}{2\pi\Lambda^4} \\ &= \left(|C_{eAL}|^2 + |C_{eAR}|^2\right) 4.32\text{fb}, \quad (10) \\ \sigma_{--} + \sigma_{++} &= \left(|C_{eAAL}|^2 + |C_{eAAR}|^2\right) \frac{v^2}{8\pi\Lambda^8} s^2 \\ &= \left(|C_{eAAL}|^2 + |C_{eAAR}|^2\right) 0.0206\text{fb},\end{aligned}$$

where the numerical value on the second line is independent of the collision energy, but the numerical value on the fourth line is taken at $\sqrt{s} = 1.095$ TeV.

Based on the same minimum cross section requirement as for the four-fermion operators, we find that the coefficients $C_{eAL(R)}$ and $C_{eAAL(R)}$ should be of order 0.1 and $\sqrt{2}$ respectively for a measurable signal.

The current limit from $\mu \to e\gamma$ is of order 5×10^{-6} for the dipole coefficient $C_{eAL(R)}$. However, for the $e\mu\gamma\gamma$ contact term coefficient $C_{eAAL(R)}$ the sensitivity from $\mu A \to eA$ transitions is six orders of magnitude less stringent: $C_{eAAL(R)} \leq 3.2$ [17]. We observe that in this case the $e\mu$ collider yields the highest sensitivity as compared to the low energy measurements.

We now perform a complete analysis of the $e^-\mu^+\gamma\gamma$ signal, taking into account the SM backgrounds, to corroborate the sensitivity estimated for $C_{eAL(R)}$ and $C_{eAAL(R)}$, for a detailed discussion we refer to Ref. [11]. First of all, we point out that, as mentioned above, the amplitudes squared for $e^-\mu^+ \to \gamma\gamma$ do not depend on the polar angle. That means that in terms of rapidity, for instance $y = y_3^*$ in the CM frame we have the differential cross section:

$$\frac{d\sigma}{dy} = \frac{d\sigma}{dc_\theta}\frac{dc_\theta}{dy} = a_0 \frac{4\exp(2y)}{(1+\exp(2y))^2} \ , \quad (11)$$

with a_0 a constant. The shape of the rapidity distribution in the CM frame is then centered around zero with a width of approximately 2 units. In the lab frame, the rapidities y are shifted with respect to those y^* in the CM frame [11]:

$$y = y^* - y_0 \ , \ \text{ with } \ y_0 = \frac{1}{2}\ln\left(\frac{E_\mu}{E_e}\right) = 1.70 \ , \quad (12)$$

where $y_0 = 1.7$ is the shift value for $E_\mu/E_e = 30$. The muon beam goes in the direction of $-\hat{k}$ and so the event products usually appear on the backwards hemisphere.

The background processes are given by $e^-\mu^+ \to \gamma\gamma\bar{\nu}_\mu\nu_e$ as well as $e^-\mu^+ \to e^-e^+\bar{\nu}_\mu\nu_e$. For illustration one diagram

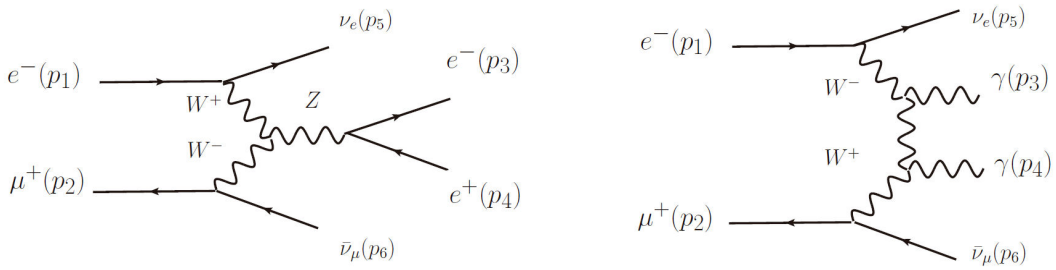

FIGURE 3. Representative diagrams for $e^-\mu^+ \to \gamma\gamma$ background processes.

for each process is shown in Fig. 3. Being two-to-four processes the γ pair should have a drastically different kinematics and be very easy to be separated from the signal γ's. In particular, we point out three clear differences: In the two-body signal process the CM $\gamma\gamma$ energies are fixed at half of the total: $E_3^* = E_4^* = \sqrt{s}/2$, whereas in the background process photon pair only part of the total energy is available and not necessarily shared equally. Regarding transverse momenta, for the signal process we have $|\vec{p}_{3T} + \vec{p}_{4T}| = 0$, but for the backgrounds $|\vec{p}_{3T} + \vec{p}_{4T}| = \not{E}_T$ which has a continuous range of values. Thirdly, the final-state photons, in the signal process, are very central in the CM frame, with $|y^*_{3,4}| = |y_{3,4} + y_0| \lesssim 2.5$ for the vast majority.

We have simulated the signal and background processes with MADGRAPH 2.6 [18], with beam energies $(E_e, E_\mu) =$ (100, 3000), (150, 4500) and (200, 6000) GeV. We then have $\sqrt{s} = 1.095$, 1.643 and 2.191 TeV, respectively.

Based on the previous considerations, we have applied the following set of phase-space cuts:

$$\begin{aligned} &C_0 : p_{3T}, p_{4T} > 1.0 \quad \text{GeV}, \\ &C_1 : E_3^*, E_4^* > 500.0 \quad \text{GeV}, \\ &C_2 : p_T^{\text{tot}} = |\vec{p}_{3T} + \vec{p}_{4T}| < 20.0 \quad \text{GeV}, \\ &C_3 : |y_3 + y_0|, |y_4 + y_0| < 1.75 \quad \text{GeV}. \end{aligned} \tag{13}$$

The cut C_0 is necessary to control infrared divergences. As expected, the cuts $C_{1,2,3}$ in Eq. (13) have negligible effects on the signal cross section, but they substantially decrease the cross section for the backgrounds.

The effect of the cuts (13) on the cross sections for the signal and background processes is illustrated at $(E_e, E_\mu) =$ (100, 3000) GeV in Table II.

The cross section $\sigma^{(3)}_{\gamma\gamma}$ refers to the signal process with only the trivalent $e\mu\gamma$ vertex and the Wilson coefficients $C_{eAL} = C_{eAR} = 1$. Similarly, $\sigma^{(4)}_{\gamma\gamma}$ refers to the signal produced by the $e\mu\gamma\gamma$ vertex and the coefficients $C_{eAAL} = C_{eAAR} = 1$. The numerical results agree with (10).

We expect the results for cross sections with cuts in Table II to be quite realistic, although detector efficiencies and acceptances have not been allowed for in those results. However, we expect the rapidity acceptance effects to be taken into account by the cut C_3 in Eq. (13), and we also expect the efficiency for photon identification to be no less than 90%, so that detector effects should be modest.

TABLE II. Cumulative effects of the cuts (13) on the cross sections for the signal and background processes at $E_e = 100$ GeV, $E_\mu = 3$ TeV. Cross sections σ given in units of fb.

$\mathcal{P}_\mu$	$\mathcal{P}_e$	cuts	$\sigma^{(3)}_{\gamma\gamma}$	$\sigma^{(4)}_{\gamma\gamma}$	$\sigma_{\nu\nu\gamma\gamma}$	$\sigma_{\nu\nu ee}$
0.0	0.0	C_0	2.16	0.0103	770.2	426.6
0.0	0.0	$C_{0,1}$	2.16	0.0103	0.0049	0.073
0.0	0.0	$C_{0\text{-}2}$	2.16	0.0103	0.0015	0.0081
0.0	0.0	$C_{0\text{-}3}$	2.04	0.0097	3×10^{-5}	0.0011
0.4	0.8	$C_{0,1}$	2.86	0.0136	0.0014	0.081
0.4	0.8	$C_{0\text{-}2}$	2.69	0.0128	0.00043	0.0082
0.4	0.8	$C_{0\text{-}3}$	2.69	0.0128	1×10^{-5}	0.0038

The important exception to this, however, is the background process $e^-\mu^+ \to e^-e^+\bar{\nu}_\mu\nu_e$ that in Table II seems to be not much smaller than $\sigma^{(4)}_{\gamma\gamma}$, but which must actually be adjusted for the electron-photon misidentification probability. In order to settle this issue, we carried out a detector simulation using Delphes 3.4 [19] and we observed a significant reduction of two orders of magnitude from the values shown in Table II once the misidentification is taken into account. For a more detailed discussion we refer the reader to Ref. [11].

4. Conclusion

In conclusion, an $e\mu$ collider would be able to provide direct evidence or limits for flavor changing $e\mu$ reactions, and with the absence of so much SM background activity, it would even become a good experiment to test flavor non-violating processes like Higgs production and decay.

Acknowledgments

We are grateful to Georgina Espinoza Gurriz for her assistance with our computer hardware. We acknowledge support from Sistema Nacional de Investigadores de Conacyt, México.

i. The scale could have been chosen to have a different value, and it is easy to translate the limits presented from one scale to another. Strictly speaking, we do not know what the actual scale of new physics is, and sometimes the bounds provided in the literature refer to the operator coefficient divided by Λ^2 in units TeV^{-2}. Sometimes Λ is set equal to 1 TeV.

ii. The common framework of the effective SM Lagrangian contains operators of dimension higher than 4. There is one possible dimension 5 operator, but it is at dimension 6 that a long list of phenomenologically relevant operators appear [13]. Then, there are a few operators of dimension 7 [15], but they do not generate the two-photon vertex of our interest. For such, we have to refer to the list of dimension 8 operators [16].

1. V. Barger, S. Pakvasa and X. Tata, Are eμ colliders interesting?, *Phys. Lett. B* **415** (1997) 200, https://doi.org/10.1016/S0370-2693(97)01234-3
2. A. Bhardwaj, C. Englert and P. Stylianou, Implications of the muon anomalous magnetic moment for the LHC and MUonE, *Phys. Rev. D* **106** (2022) 075031, https://doi.org/10.1103/PhysRevD.106.075031
3. S. Y. Choi *et al.*, High-energy FCNC search through eμ colliders, *Phys. Rev. D* **57** (1998) 7023, https://doi.org/10.1103/PhysRevD.57.7023
4. J. C. Montero, V. Pleitez and M. C. Rodriguez, Left-right asymmetries in polarized e - μ scattering, *Phys. Rev. D* **58** (1998) 097505, https://doi.org/10.1103/PhysRevD.58.097505
5. G. Cvetič and C. S. Kim, Heavy Majorana neutrino production at electron - muon colliders, *Phys. Lett. B* **461** (1999) 248, [erratum: *Phys. Lett. B* **471** (2000) 471], https://doi.org/10.1016/S0370-2693(99)00848-5
6. F. Almeida *et al.*, Single neutral heavy lepton production at electron-muon colliders, *Phys. Lett. B* **494** (2000) 273, https://doi.org/10.1016/S0370-2693(00)01195-3
7. J. K. Singhal, S. Singh, and A. K. Nagawat, Possible exotic neutrino signature in electron muon collisions (2007), https://doi.org/10.48550/arXiv.hep-ph/0703136
8. M. Casarsa, Prospects of a future multi-TeV muon collider, *SciPost Phys. Proc.* **8** (2022) 061, https://doi.org/10.21468/SciPostPhysProc.8.061
9. F. Bossi, and P. Ciafaloni, Lepton Flavor Violation at muon-electron colliders, *JHEP* **2020** (2020) 33, https://doi.org/10.1007/JHEP10(2020)033
10. M. Lu, *et al.*, The physics case for an electron-muon collider, *Adv. High Energy Phys.* **2021** (2021) 6693618, https://doi.org/10.1155/2021/6693618
11. A. O. Bouzas, and F. Larios, Two-to-Two Processes at an Electron-Muon Collider, *Adv. High Energy Phys.* **2022** (2022) 3603613, https://doi.org/10.1155/2022/3603613
12. S. Davidson, Completeness and complementarity for $\mu \to e\gamma\mu \to e\bar{e}e$ and $\mu A \to eA$, *JHEP* **2021** (2021) 172, https://doi.org/10.1007/JHEP02(2021)172
13. B. Grzadkowski et al., Dimension-six terms in the Standard Model Lagrangian, *JHEP* **10** (2010) 085, https://doi.org/10.1007/JHEP10(2010)085
14. M. Ardu, and S. Davidson, What is Leading Order for LFV in SMEFT?, *JHEP* **2021** (2021) 2, https://doi.org/10.1007/JHEP08(2021)002
15. L. Lehman, Extending the Standard Model Effective Field Theory with the Complete Set of Dimension-7 Operators, *Phys. Rev. D* **90** (2014) 125023, https://doi.org/10.1103/PhysRevD.90.125023
16. Li, Hao-Lin and Ren, Zhe and Shu, Jing and Xiao, Ming-Lei and Yu, Jiang-Hao and Zheng, Yu-Hui, Complete set of dimension-eight operators in the standard model effective field theory, *Phys. Rev. D* **104** (2021) 015026, https://doi.org/10.1103/PhysRevD.104.015026
17. S. Davidson, and Y. Kuno, and Y. Uesaka, and M. Yamanaka, Probing $\mu e\gamma\gamma$ contact interactions with $\mu \to e$ conversion, *Phys. Rev. D* **102** (2020) 115043, https://doi.org/10.1103/PhysRevD.102.115043
18. J. Alwall *et al.*, MadGraph 5: Going Beyond, *JHEP* **06** (2011) 128, https://doi.org/10.1007/JHEP06(2011)128
19. J. De Favereau *et al.*, DELPHES 3, A modular framework for the fast simulation of a generic collider experiment, *JHEP* **2014** (2014) 57, https://doi.org/10.1007/JHEP02(2014)057